JBC ARTICLE

A comprehensive analysis of Rab GTPases reveals a role for Rab34 in serum starvation-induced primary ciliogenesis

Received for publication, December 7, 2019, and in revised form, July 14, 2020 Published, Papers in Press, July 15, 2020, DOI 10.1074/jbc.RA119.012233

Mai E. Oguchi, Koki Okuyama, Yuta Homma, and Mitsunori Fukuda*

From the Laboratory of Membrane Trafficking Mechanisms, Department of Integrative Life Sciences, Graduate School of Life Sciences, Tohoku University, Aobayama, Aoba-ku, Sendai, Miyagi, Japan

Edited by Enrique M. De La Cruz

Primary cilia are sensors of chemical and mechanical signals in the extracellular environment. The formation of primary cilia (*i.e.* ciliogenesis) requires dynamic membrane trafficking events, and several Rab small GTPases, key regulators of membrane trafficking, have recently been reported to participate in ciliogenesis. However, the precise mechanisms of Rab-mediated membrane trafficking during ciliogenesis remain largely unknown. In the present study, we used a collection of siRNAs against 62 human Rabs to perform a comprehensive knockdown screening for Rabs that regulate serum starvation-induced ciliogenesis in human telomerase reverse transcriptase retinal pigment epithelium 1 (hTERT-RPE1) cells and succeeded in identifying Rab34 as an essential Rab. Knockout (KO) of Rab34, but not of Rabs previously reported to regulate ciliogenesis (*e.g.* Rab8 and Rab10) in hTERT-RPE1 cells, drastically impaired serum starvation-induced ciliogenesis. Rab34 was also required for serum starvation-induced ciliogenesis in NIH/3T3 cells and MCF10A cells but not for ciliogenesis in Madin-Darby canine kidney (MDCK)-II cysts. We then attempted to identify a specific region(s) of Rab34 that is essential for ciliogenesis by performing deletion and mutation analyses of Rab34. Unexpectedly, instead of a specific sequence in the switch II region, which is generally important for recognizing effector proteins (*e.g.* Rab interacting lysosomal protein [RILP]), a unique long N-terminal region of Rab34 before the conserved GTPase domain was found to be essential. These findings suggest that Rab34 is an atypical Rab that regulates serum starvation-induced ciliogenesis through its unique N-terminal region.

Primary cilia are membrane projections from the cell surface and are thought to function as sensors of chemical and mechanical signals in the extracellular environment (1). Defects in the formation or function of primary cilia cause various human diseases called ciliopathies (2). The assembly and disassembly of primary cilia are tightly coupled to cell cycle progression, and primary cilia form in cells in the resting stage (3). Primary cilium formation (so-called ciliogenesis) is known to occur in a series of membrane-trafficking steps (4–6). First, small vesicles, called preciliary vesicles, accumulate on the mother centriole, and then the preciliary vesicles fuse with each other to form a large vesicle called a ciliary vesicle. The resulting ciliary vesicle extends together with the axoneme and finally fuses with the plasma membrane. It is generally thought that lipids and ciliary proteins must be transported from other organelles, such as the Golgi apparatus and recycling endosomes, to the mother centriole via membrane trafficking mechanisms during the ciliary vesicle formation and elongation (7, 8).

Rab small GTPases, which belong to the Ras superfamily, are key regulators of membrane trafficking (9–12). Rabs function as switch proteins that cycle between an active state and an inactive state. In their active state, Rabs localize to specific vesicles or organelles and recruit a specific binding partner (called a Rab effector), via which they regulate a specific membrane trafficking pathway. Recent studies have reported that several Rabs, including Rab8, Rab10, Rab11, Rab23, Rab29, and Rab34, participate in ciliogenesis (8, 13–18). However, not all of the membrane trafficking mechanisms in ciliogenesis are fully understood, and knockout mice in which each of several cilia-regulating Rabs had been knocked out did not exhibit any ciliopathy phenotypes (15, 19). Moreover, no attempts have been made to perform a comprehensive analysis of all mammalian Rabs (Rab1A–43) during ciliogenesis.

In this study, we performed a comprehensive knockdown screening for Rabs that regulate serum starvation-induced ciliogenesis in hTERT-RPE1 (human telomerase reverse transcriptase retinal pigment epithelium 1) cells and succeeded in identifying Rab34 as an essential Rab in serum starvation-induced ciliogenesis. Intriguingly, however, the known cilia-regulating Rabs, including Rab8, Rab10, Rab11B, and Rab12, were found to be dispensable for ciliogenesis, because their knockout (KO) cells formed primary cilia. Moreover, the requirement of Rab34 for serum starvation-induced ciliogenesis was confirmed in NIH/3T3 cells and MCF10A cells. On the other hand, Rab34 was not essential for ciliogenesis in cysts of Madin-Darby canine kidney (MDCK)-II cells. We then performed KO-rescue experiments on several Rab34 mutants, including a switch II swapping mutant (S1A) and an N-terminal deletion mutant (ΔN), to identify the region of Rab34 that is responsible for ciliogenesis. The results showed that Rab34(S1A) rescued the Rab34-KO phenotype but that Rab34 (ΔN) did not. These findings indicate that the unique long N-terminal region of Rab34, and not a specific sequence in the switch II region, is necessary for serum starvation-induced ciliogenesis.

Results

Comprehensive screening for Rabs whose knockdown inhibits ciliogenesis in hTERT-RPE1 cells

To identify novel Rabs that participate in serum starvation-induced primary ciliogenesis, by using effective and specific

This article contains supporting information.
* For correspondence: Mitsunori Fukuda, nori@tohoku.ac.jp.

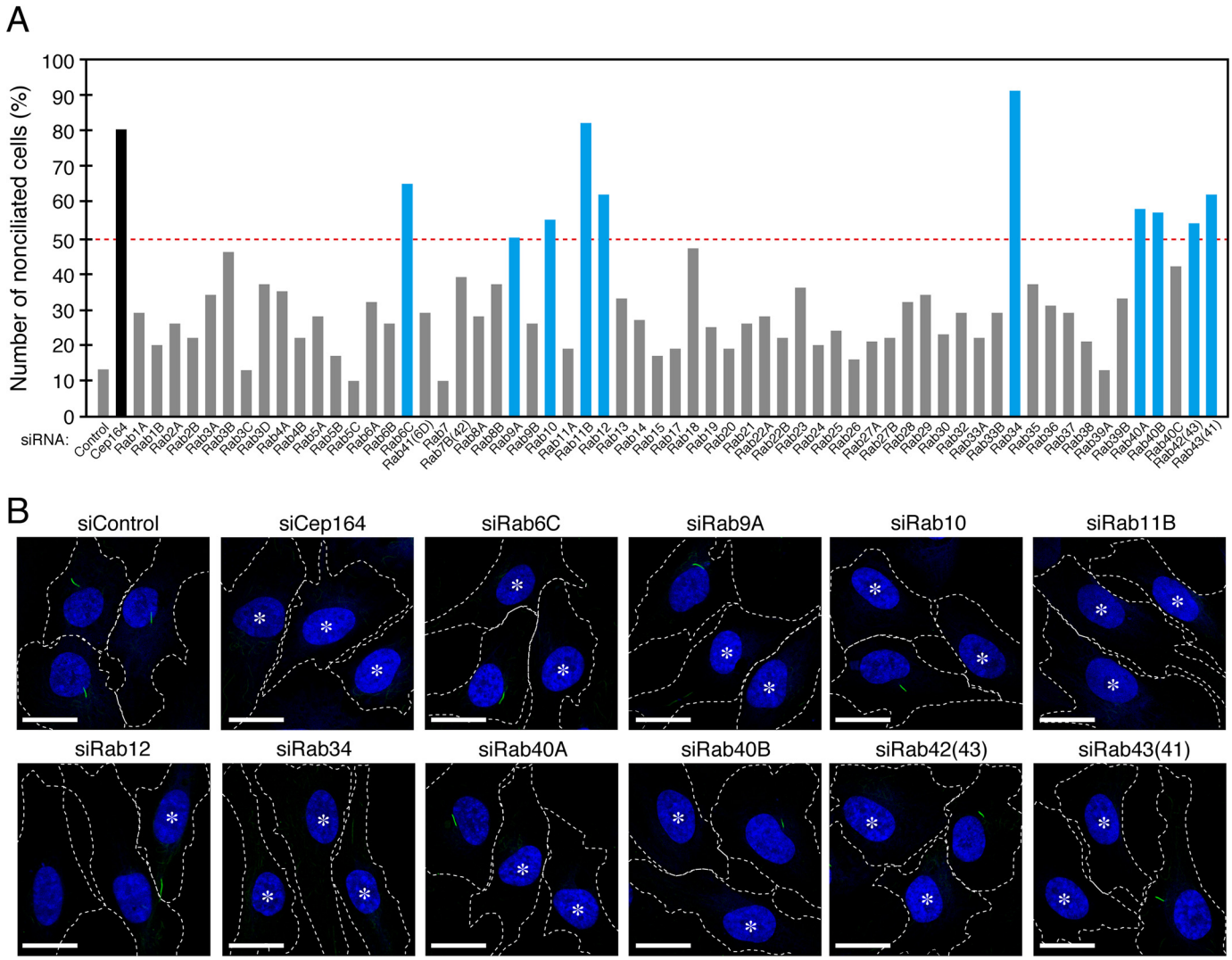

Figure 1. Screening for Rabs whose knockdown inhibited ciliogenesis in hTERT-RPE1 cells. *A*, the number of nonciliated hTERT-RPE1 cells (%) that have been transfected with siRNA against each Rab isoform (0.2 nM) was counted after a 24-h serum starvation ($n > 50$ cells). The *broken red line* indicates that 50% of the cells have no cilia. The *black bar* represents Cep164 (positive control), and the *blue bars* represent candidate Rabs whose knockdown increased the number of nonciliated cells to more than 50% compared with the control siRNA (negative control). Because of the high sequence identity between Rab40A and Rab40AL, *Rab40A* siRNA was also able to knock down Rab40AL (20). *B*, typical images of cells transfected with control siRNA (*siControl*), *Cep164* siRNA (*siCep164*) (positive control), or siRNA against candidate Rabs (*siRab*). The cells were fixed after a 24-h serum starvation and then stained with anti-acetylated tubulin antibody (*green*; cilia) and DAPI (*blue*; nuclei). The *broken white lines* indicate the boundaries of each cell. *, nonciliated cells. *Scale bars*, 20 μm.

siRNAs against 62 human Rabs that we have developed previously (20), we performed a comprehensive knockdown screening in hTERT-RPE1 cells. We used acetylated tubulin as a cilium marker and then counted the number of nonciliated cells. When we knocked down CEP164 protein that is essential for ciliogenesis (21), the number of nonciliated cells increased to more than 80% (Fig. 1*A*, *black bar*), whereas control siRNA had almost no effect (~10% of the cells were nonciliated), thereby validating our experimental setup. The results of the screening showed that knockdown of ten Rabs, *i.e.* Rab6C, Rab9A, Rab10, Rab11B, Rab12, Rab34, Rab40A, Rab40B, Rab42(43), and Rab43(41), increased the number of nonciliated cells to more than 50% (Fig. 1*A*, *blue bars*, and *B*), and we considered these Rabs to be primary candidates.

To confirm the knockdown effects on ciliogenesis that had been observed in the first screening and to avoid possible off-target effects by single siRNAs, we proceeded to perform knockdown experiments by using other independent siRNAs against the primary Rab candidates. The results showed that knockdown of only four Rabs, *i.e.* Rab6C, Rab11B, Rab12, and Rab34, by each of two independent siRNAs increased the number of nonciliated cells to more than 50% (Fig. 2*A*). We also checked the protein expression levels of several candidate Rabs by immunoblotting, and the results confirmed that the Rab11B, Rab12, and Rab34 bands almost completely disappeared when the two independent siRNAs were used (Fig. 2*B*). siRab9A#2 and siRab10#2 seemed to decrease the protein expression level more efficiently than siRab9A#1 and siRab10#1, respectively (Fig. 2*B* and data not shown), but they had a lesser effect on ciliogenesis, suggesting that siRab9A#1 and siRab10#1 have certain off-target effects on ciliogenesis. On the other hand, no protein expression of other candidate Rabs, including Rab6C,

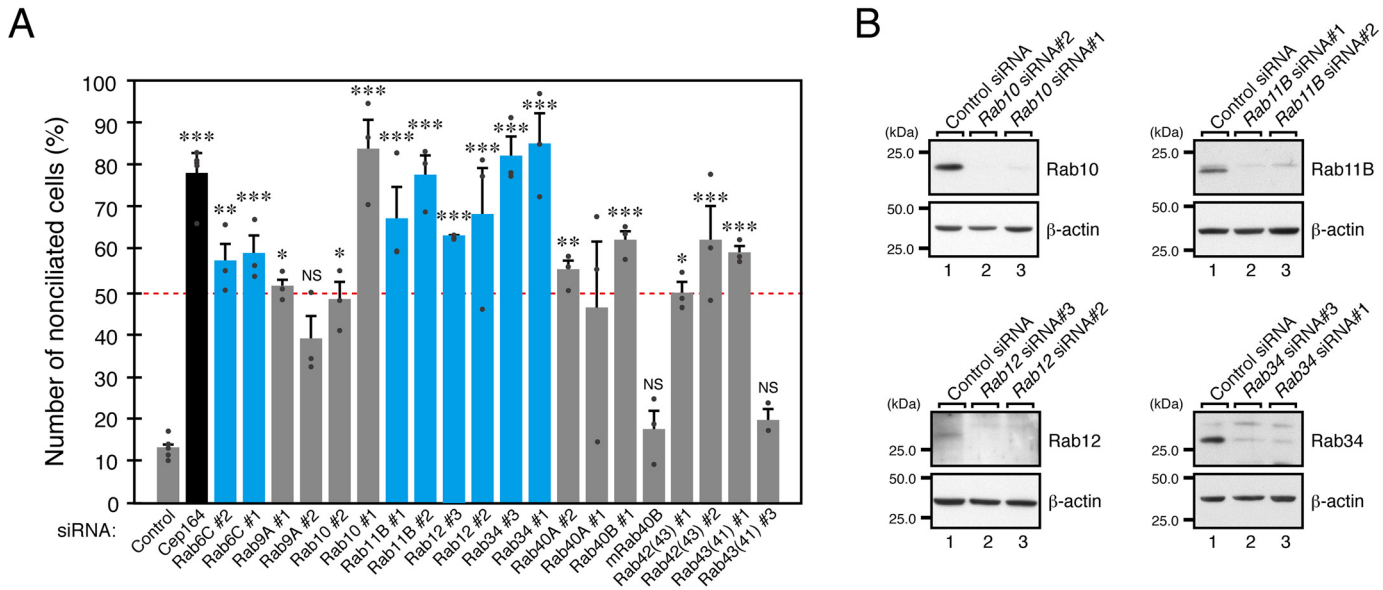

Figure 2. Secondary screening for Rabs whose knockdown inhibited ciliogenesis by using another siRNA site. *A*, the number of nonciliated hTERT-RPE1 cells (%) transfected with the siRNAs (0.2 nM) indicated was counted after a 24-h serum starvation ($n > 50$ cells). *Error bars* indicate the S.E. of data from three independent experiments. The *broken red line* indicates that 50% of the cells have no cilia. The *black bar* represents Cep164 (positive control), and the *blue bars* represent candidate Rabs whose knockdown with two independent siRNAs increased the number of nonciliated cells to more than 50% compared with the control siRNA (negative control). *, $p < 0.05$; **, $p < 0.01$; ***, $p < 0.001$; NS, not significant compared with the control siRNA (Tukey's test). *B*, the knockdown efficiency of candidate Rabs was evaluated by immunoblotting with the antibodies indicated on the *right* of each panel. Cells were harvested 48 h after transfection with control siRNA or siRNA against candidate Rabs (0.2 nM). *Lane 1* and *lanes 2* and *3* show the results for the control siRNA and for two independent siRNAs against each Rab, respectively. The positions of the molecular mass markers (in kDa) are shown on the left.

was detected by immunoblotting (data not shown), and we did not pursue Rab6C in the subsequent analysis. Based on the results of the two-step screenings, we selected Rab11B, Rab12, and Rab34 as secondary candidate Rabs.

A possible function of Rab11 in ciliogenesis had already been reported (8), but involvement of Rab12 and Rab34 in ciliogenesis had not been investigated by the time we completed the comprehensive screening. During investigating Rab12 and Rab34 in the subsequent analysis, their possible involvement in ciliogenesis was reported by other groups (17, 22–24), although the detailed molecular mechanisms remained unknown.

Rab34 is required for ciliogenesis in hTERT-RPE1 cells

To determine whether the secondary candidates identified above, *i.e.* Rab11B, Rab12, and Rab34, are indeed essential for ciliogenesis in hTERT-RPE1 cells, we generated their respective KO cells by using the CRISPR/Cas9 system. We also established Rab8A/B-double KO (Rab8A/B-KO) cells and Rab8A/B/10-triple KO (Rab8A/B/10-KO) cells as controls, because Rab8 and Rab10 are widely thought to be involved in cilium formation in mammalian cultured cells (15). Loss of the target Rabs in each KO cell was verified by both immunoblotting (Fig. 3*B*) and sequencing of genomic PCR products (Fig. S1). As shown in Fig. 3*A*, only Rab34-KO greatly increased the number of nonciliated cells. In contrast, Rab8A/B-KO, Rab10-KO, Rab8A/B/10-KO, Rab11B-KO, and Rab12-KO cells did not show any defects in ciliogenesis under our experimental conditions. The KO phenotypes observed in this study are unlikely to be caused by clonal variations, because essentially the same results were obtained in other independent Rab-KO clones (*i.e.* impaired ciliogenesis in Rab34-KO cells *versus* normal ciliogenesis in other Rab-KO cells) (data not shown).

To further confirm that the impaired ciliogenesis was directly related to Rab34-KO, we performed rescue experiments by stably expressing EGFP (enhanced GFP)-P2A-Rab34, which contains a P2A self-cleavage site (25) between EGFP and Rab34, in Rab34-KO cells (Fig. S2*A*). The results showed that expression of EGFP-P2A-Rab34 completely rescued the impaired ciliogenesis phenotype of Rab34-KO cells (Fig. 3, *C* and *D*). We used EGFP-P2A-Rab34 instead of EGFP-Rab34 for the KO-rescue experiment, because EGFP-P2A-Rab34 was able to rescue the phenotype of Rab34-knockdown (KD) cells more efficiently than EGFP-Rab34 was (Fig. S2*B*), suggesting that N-terminal EGFP tagging partly distorts the function of Rab34. A similar observation was previously reported with respect to Rab10: untagged Rab10, but not EGFP-Rab10, was found to promote neurite outgrowth of Rab10-depleted cells (26). These findings suggest that Rab34 is the most crucial Rab for serum starvation-induced ciliogenesis in hTERT-RPE1 cells.

Requirement of Rab34 for ciliogenesis depends on the cell type

To determine whether Rab34 is a general positive regulator of ciliogenesis, we investigated the effect of Rab34-KO or -KD on ciliogenesis in other cell types. As shown in Fig. 4, *A* and *B*, Rab34 depletion in NIH/3T3 cells and MCF10A cells resulted in an increase in the number of nonciliated cells under serum-starved conditions, the same as that in hTERT-RPE1 cells, and the impaired ciliogenesis of Rab34-KO NIH/3T3 cells and Rab34-KD MCF10A cells was clearly rescued by expression of EGFP-P2A-Rab34. On the other hand, checking the primary cilia in the cysts of Rab-KO MDCK-II cells that we recently established (27)

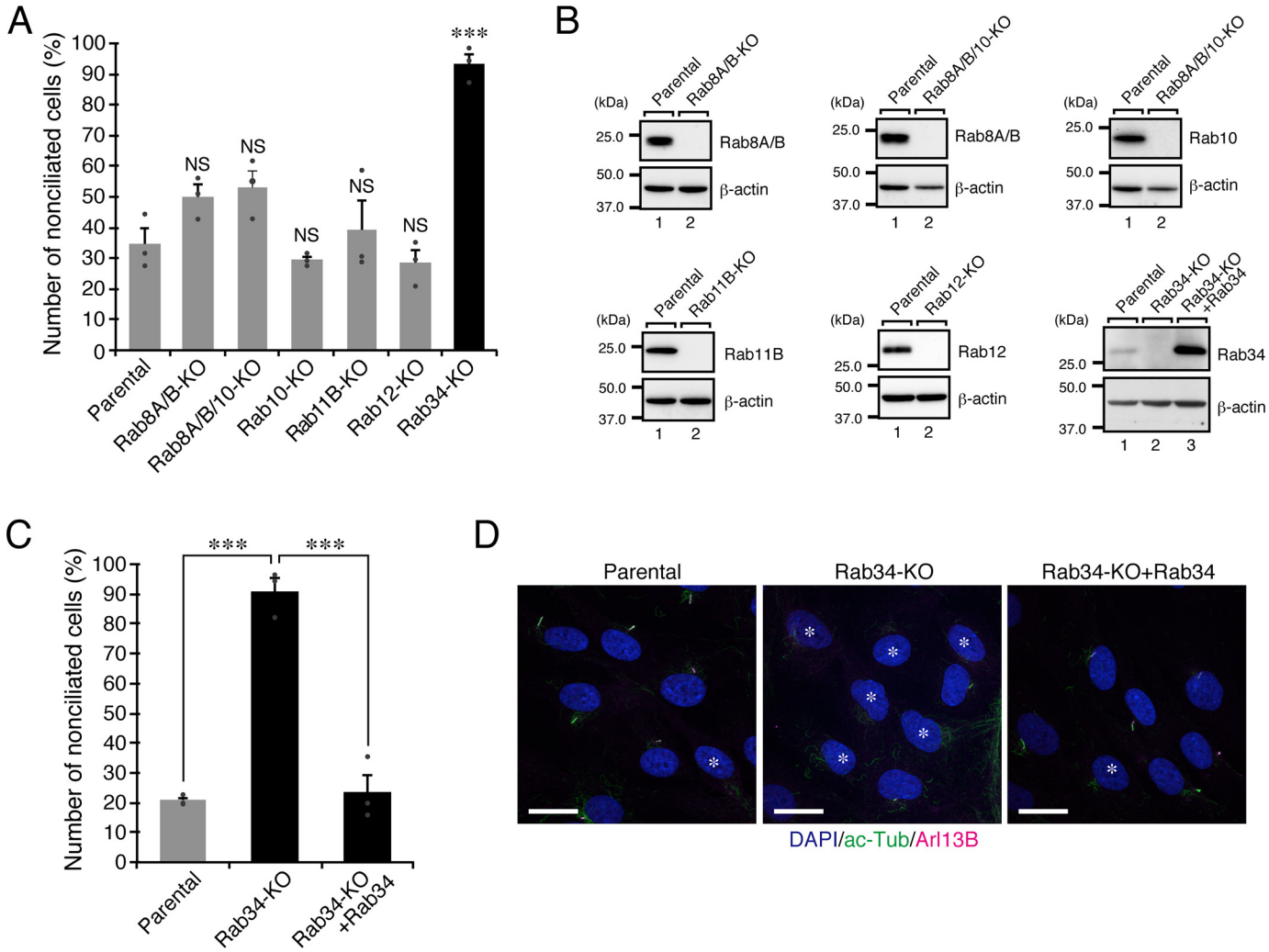

Figure 3. Rab34 is required for ciliogenesis in hTERT-RPE1 cells. *A*, the number of nonciliated cells (%) in parental, Rab8A/B-KO, Rab10-KO, Rab8A/B/10-KO, Rab11B-KO, Rab12-KO, and Rab34-KO cells was counted after a 24-h serum starvation ($n > 50$ cells). *Error bars* indicate the S.E. of data from three independent experiments. ***, $p < 0.001$; *NS*, not significant (Dunnett's test). *B*, the loss of Rab8A/B, Rab10, Rab11B, Rab12, or Rab34 in respective KO cells was analyzed by immunoblotting with the antibodies indicated on the *right* of each panel. The positions of the molecular mass markers (in kDa) are shown on the *left*. *C*, the number of nonciliated cells (%) in parental, Rab34-KO, and stable EGFP-P2A-Rab34-expressing Rab34-KO (*Rab34-KO + Rab34*) cells was counted after a 24-h serum starvation ($n > 50$ cells). *Error bars* indicate the S.E. of data from three independent experiments. ***, $p < 0.001$ (Tukey's test). *D*, typical images of parental, Rab34-KO, and Rab34-KO + Rab34 cells. The cells were fixed after a 24-h serum starvation and then stained with anti-acetylated tubulin antibody (*ac-Tub*, in *green*; cilia), anti-Arl13B antibody (*magenta*; cilia), and DAPI (*blue*; nuclei). *, nonciliated cells. *Scale bars*, 20 μm.

revealed that all of the Rab-KO cysts, including the Rab34-KO cysts, had formed primary cilia in their luminal domain (Fig. 4*C* and Fig. S3). Although Rab6 and Rab11 have been shown to be required for normal epithelial morphogenesis (27), their KO cysts still had primary cilia in their luminal domain (Fig. 4*D*). Thus, Rab34 is unlikely to be a general regulator of ciliogenesis, and it is dispensable for ciliogenesis at least in MDCK-II cysts.

Rab34 is required for early steps in serum starvation-induced ciliogenesis in hTERT-RPE1 cells

To investigate the defective ciliogenesis in the absence of Rab34 in greater detail, we then investigated the subcellular localization of ciliary membrane proteins and proteins that are required for ciliogenesis, *i.e.* Rabin8, CP110, IFT20, and Arl13B (7, 14, 28, 29), in Rab34-KO cells. As shown in Fig. 5*A*, Rab34-KO had no effect on the localization of Rabin8 (3 h after serum starvation) or of CP110, IFT20, and Arl13B (24 h after serum starvation) in hTERT-RPE1 cells compared with that of the control parental cells for removal of CP110 from mother centrioles (Fig. 5*A*, *arrows* in the *second row*) (28), and the centriole localization of Rabin8, IFT20, and Arl13B (Fig. 5*A*, *arrowheads* in the *top*, *third*, and *bottom rows*, respectively). Essentially the same results were reported for CP110, Rabin8, and IFT20 in Rab34-KO NIH/3T3 cells (23), indicating that Rab34 is not involved in the recruitment of Rabin8 and IFT20 to centrioles or CP110 removal. Because depletion of Rab34 inhibited the axoneme elongation and extension of ciliary vesicles, Rab34 is likely to be required for early steps in serum starvation-induced ciliogenesis in hTERT-RPE1 cells.

Because our anti-Rab34 antibody was unable to detect the subcellular localization of endogenous Rab34 in hTERT-RPE1 cells by immunofluorescence analysis, we tried overexpressing FLAG-tagged Rab34, which can restore the Rab34-KO

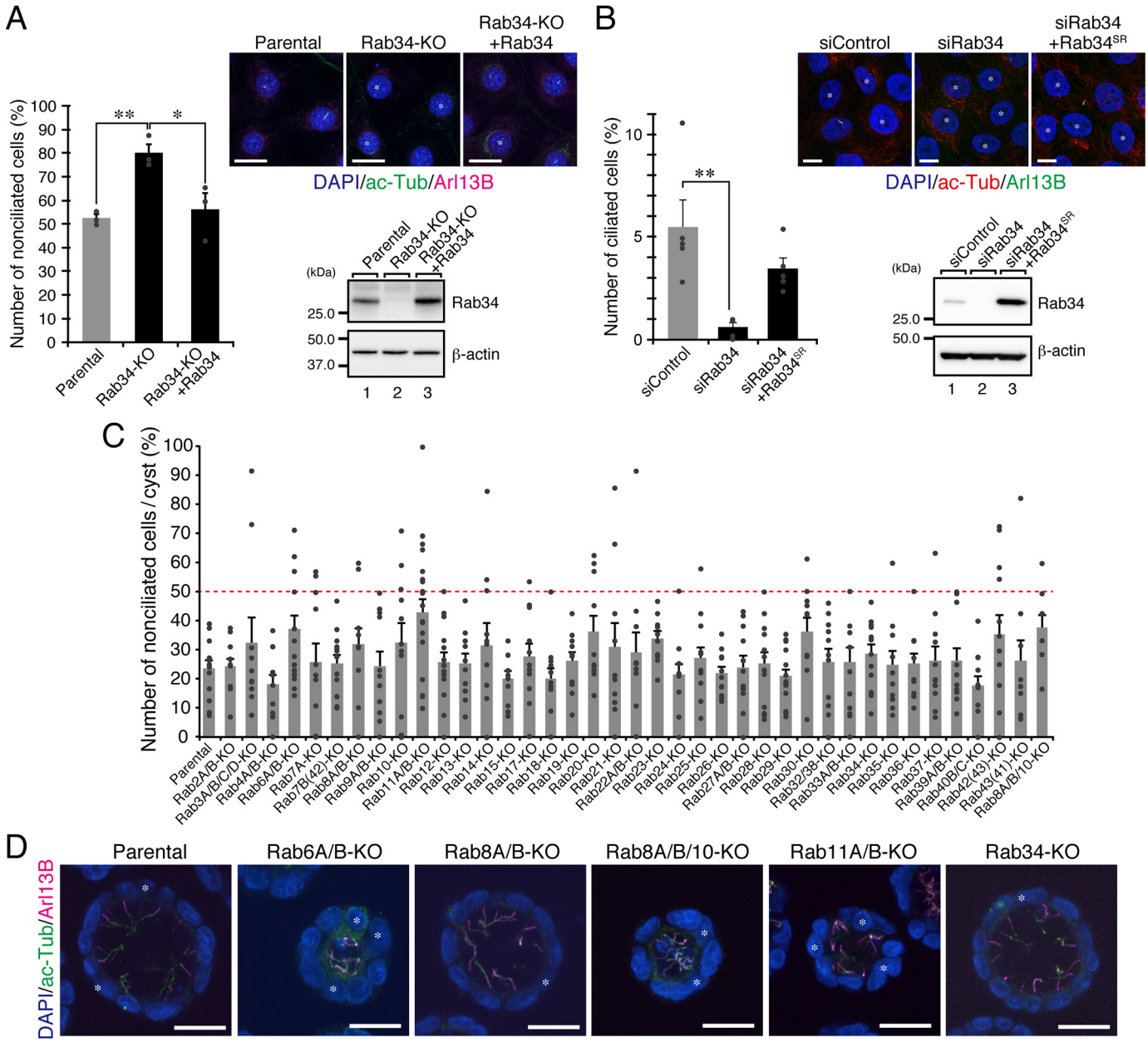

Figure 4. Rab34 is also required for ciliogenesis in NIH/3T3 cells and MCF10A cells but not in MDCK-II cells. *A*, the number of nonciliated cells (%) in the parental, Rab34-KO, and stable EGFP-P2A-Rab34-expressing Rab34-KO (*Rab34-KO + Rab34*) NIH/3T3 cells was counted after a 48-h serum starvation ($n > 50$ cells). *Error bars* indicate the S.E. of data from three independent experiments. *, $p < 0.05$; **, $p < 0.01$ (Tukey's test). Typical images of parental, Rab34-KO, and Rab34-KO + Rab34 cells are shown. The cells were fixed after a 48-h serum starvation and then stained with anti-acetylated tubulin antibody (*ac-Tub*, in *green*; cilia), anti-Arl13B antibody (*magenta*; cilia), and DAPI (*blue*; nuclei). *, nonciliated cells. *Scale bars*, 20 μm. The loss of Rab34 in KO cells was confirmed by immunoblotting with the antibodies indicated on the *right* of each panel. The positions of the molecular mass markers (in kDa) are shown on the *left*. *B*, the number of ciliated cells (%) in the control (*siControl*), Rab34-KD (*siRab34*), and stable EGFP-P2A-Rab34-expressing Rab34-KD (*siRab34 + Rab34*) MCF10A cells was counted after a 24-h serum starvation ($n > 500$ cells). *Error bars* indicate the S.E. of data from five independent experiments. **, $p < 0.01$ (Tukey's test). The cells were fixed after a 24-h serum starvation and then stained with anti-acetylated tubulin antibody (*ac-Tub*, in *red*; cilia), anti-Arl13B antibody (*green*; cilia), and DAPI (*blue*; nuclei). *, nonciliated cells. *Scale bars*, 10 μm. The knockdown efficiency of Rab34 was evaluated by immunoblotting with the antibodies indicated on the *right* of each panel. Cells were harvested 72 h after transfection with control siRNA (*siControl*) or Rab34 siRNA (*siRab34*). The positions of the molecular mass markers (in kDa) are shown on the *left*. *C*, the number of nonciliated cells per cyst (%) in parental and Rab-KO MDCK-II cells was counted after a 7-day culture in collagen gel. Note that the percentage of nonciliated cells of all of the Rab-KO cysts was below 50% (indicated as a *broken red line*). *Error bars* indicate the S.E. of data from at least ten cysts. *D*, typical images of parental, Rab6A/B-KO, Rab8A/B-KO, Rab8A/B/10-KO, Rab11A/B-KO, and Rab34-KO MDCK-II cells. The cells were fixed after a 7-day culture in collagen gel and then stained with anti-acetylated tubulin antibody (*ac-Tub*, in *green*; cilia), anti-Arl13B antibody (*magenta*; cilia), and DAPI (*blue*; nuclei). *, nonciliated cells. *Scale bars*, 20 μm.

phenotype in Rab34-KO cells (Fig. 6*E*), and visualized it by using an anti-FLAG tag antibody. The results showed that FLAG-Rab34 was mainly localized at the Golgi apparatus, consistent with the findings in a previous report (30), and that it rarely localized at primary cilia (~20%) (Fig. 5*B*). Taken together, these results imply that Rab34, an early-step regulator of ciliogenesis, is released from ciliary membranes before the maturation of primary cilia.

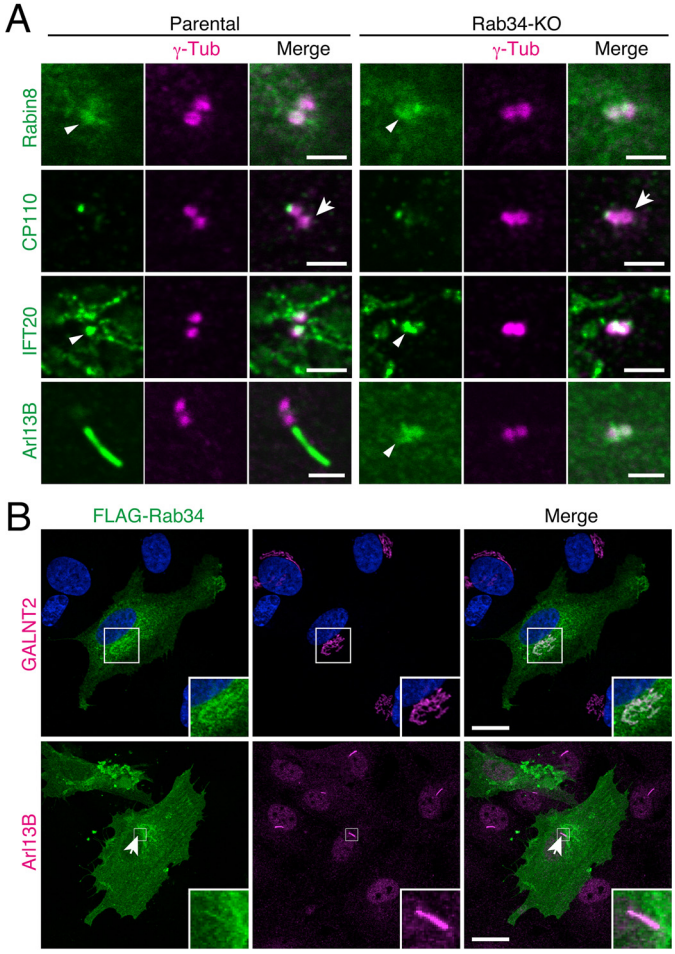

Figure 5. Rab34 is required for early steps in serum starvation-induced ciliogenesis in hTERT-RPE1 cells. *A*, typical Rabin8, CP110, IFT20, and Arl13B images of parental and Rab34-KO cells. *Top row*, for Rabin8 staining, cells stably expressing EGFP-Rabin8 (*green*) were fixed after a 1-h serum starvation and then stained with anti-γ-tubulin antibody (γ-*Tub*, in *magenta*; centrioles). For CP110, IFT20, and Arl13B staining, cells were fixed after a 24-h serum starvation and then stained with antibodies against CP110 (*green*) and γ-tubulin (*magenta*) (*second row*), IFT20 (*green*) and γ-tubulin (*magenta*) (*third row*), or Arl13B (*green*) and γ-tubulin (*magenta*) (*bottom row*). The *arrows* and *arrowheads* indicate CP110-negative centrioles and centriole-localized Rabin8 (IFT20 or Arl13B), respectively. *Scale bars*, 2 μm. *B*, typical images of FLAG-Rab34 and GALNT2 or Arl13B in hTERT-RPE1 cells expressing FLAG-Rab34(WT). *Top*, for GALNT2 staining, cells were fixed without serum starvation and stained with antibodies against GALNT2 (*magenta*) and FLAG (*green*). *Bottom*, for Arl13B staining, cells were fixed after a 24-h serum starvation and then stained with antibodies against Arl13B (*magenta*) and FLAG (*green*). The arrows indicate FLAG-Rab34-positive primary cilia. *Scale bars*, 20 μm.

The unique long N-terminal region of Rab34 is required for ciliogenesis in hTERT-RPE1 cells

Next, we attempted to identify a specific region(s) of Rab34 that is essential for ciliogenesis by performing mutation and deletion analyses of Rab34-KO cells. In general, Rabs are thought to recognize specific effectors through their switch II region, because mutations of specific amino acids in this region of some Rabs have been shown to abrogate their effector-binding ability (31–35). Sequence comparisons of the switch II region of mammalian Rabs have revealed that Lys-115 and Cys-116 are specific to Rab34 (and its closest paralog, Rab36) (Fig. 6*A*, *asterisks*) (34). Actually, we had previously shown that K120A/C121A mutations of Rab36 impaired RILP (Rab interacting lysosomal protein)-binding activity, and that the Rab36 (K120A/C121A) mutant did not support retrograde melanosome transport in melanocytes (34). Therefore, we generated a Rab34(K115A/C116A) [here referred to as Rab34 (KC/AA)] mutant and evaluated its effect on ciliogenesis in Rab34-KD hTERT-RPE1 cells.

Consistent with the previous finding regarding Rab36 (34), Rab34(KC/AA) failed to interact with RILP in yeast two-hybrid assays (Fig. S4*A*) and was shown to hardly interact with it by coimmunoprecipitation assays (Fig. S4*B*). Unexpectedly, however, Rab34(KC/AA) completely rescued the Rab34-KD phenotype (Fig. S4*C*). Because a weak interaction between Rab34(KC/AA) and RILP was still observed in the coimmunoprecipitation assays (Fig. S4*B*), it was possible that such a weak interaction could rescue the KD phenotype. To rule out this possibility, we generated an additional Rab34 mutant that completely lacks RILP-binding ability by swapping the switch II region of Rab34 for that of Rab1A, a Rab isoform distantly related to Rab34 [named Rab34(S1A)] (Fig. 6*A*), and complete loss of RILP-binding activity by Rab34(S1A) was confirmed by both yeast two-hybrid assays and coimmunoprecipitation assays (Fig. 6, *B* and *C*). Nevertheless, Rab34(S1A) did rescue the Rab34-KO phenotype, the same as Rab34(WT) did (Fig. 6*D*). Although no specific sequence in the switch II region of Rab34 was essential for ciliogenesis, GTP-binding activity of Rab34 itself was necessary, because a constitutively active Rab34 mutant, Rab34(Q111L), but not its constitutively inactive mutant, Rab34(T66N), rescued the Rab34-KD effect on ciliogenesis, as did Rab34(WT) (Fig. S5).

To further identify the crucial region of Rab34 for ciliogenesis, we compared the entire sequences of mammalian Rab family members in greater detail and discovered that Rab34 contains a long N-terminal region (*gray box* in Fig. 6*A*) that was not found in other Rab isoforms except Rab36. Rab36, the closest paralog of Rab34, also contains a long N-terminal sequence, but the N-terminal sequences are not well conserved between them. Therefore, we produced an N-terminal deletion mutant of Rab34 [named Rab34(ΔN)], which lacks the 49 N-terminal amino acids of Rab34, and performed a rescue experiment. The results showed that Rab34(ΔN) did not rescue the Rab34-KO phenotype at all (Fig. 6*E*). The lack of a rescue effect by Rab34 (ΔN) is unlikely to be attributable to its protein expression level, because similar amounts of Rab34(ΔN) and endogenous Rab34 were observed in hTERT-RPE1 cells (Fig. 6*F*). Moreover, FLAG-tagged Rab34(S1A) and Rab34(ΔN) mainly localized at the Golgi apparatus, the same as Rab34(WT) did (Fig. 6*G* and 5*B*). It should be noted that Rab34(S1A) localized at primary cilia to an extent similar to that of Rab34(WT) (~20%), whereas we did not observe any ciliary localization of Rab34(ΔN) under our experimental conditions. Thus, the unique N-terminal region of Rab34 is not involved in its Golgi localization, but it may be required for its ciliary targeting or localization. However, because the protein expression level of Rab34(ΔN) was often lower than that of Rab34(WT) and Rab34(S1A) (Figs. 3*B* and 6*F*), we could not completely rule out the possibility that its low protein expression masked the ciliary localization of Rab34 (ΔN).

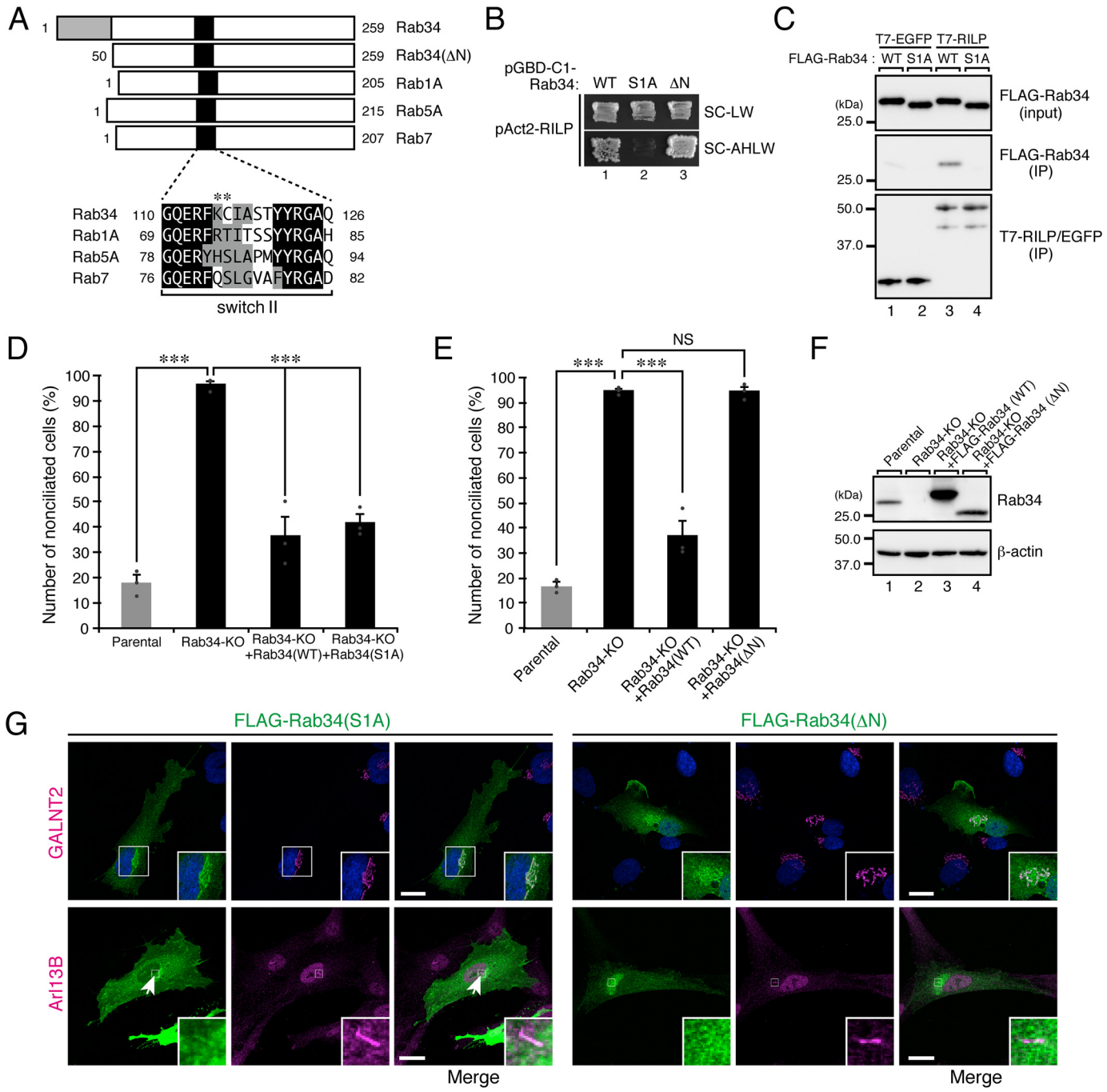

Figure 6. The unique long N-terminal region of Rab34, not its specific sequence in the switch II region, is required for ciliogenesis in hTERT-RPE1 cells. *A*, schematic representation of mouse Rab1A, Rab5A, Rab7, and Rab34 (WT and ΔN) and sequence alignment of the switch II region (*black boxes*) of mouse Rab1A, Rab5A, Rab7, and Rab34. Identical and similar residues in the switch II region are shown against a *black background* and a *gray background*, respectively. Lys-115 and Cys-116 of Rab34 (*asterisks*) are not conserved in other Rabs except Rab36 (34) (see also Fig. S4). The unique long N-terminal region of Rab34 is indicated by a *gray box*. *B*, interaction between Rab34(WT), Rab34(S1A), or Rab34(ΔN) and RILP was analyzed by yeast two-hybrid assays. Yeast cells expressing pGBD-C1-Rab34 (WT), Rab34(S1A), or Rab34(ΔN) and pAct2-RILP were streaked on an SC-LW plate (*upper*) and on an SC-AHLW plate (*lower*, selection medium) and incubated at 30 °C. *C*, interaction between Rab34(WT) or Rab34(S1A) and RILP was analyzed by coimmunoprecipitation assays of COS7 cell lysates. COS7 cell lysates expressing FLAG-tagged Rab34(WT) or Rab34(S1A) and T7-tagged EGFP or RILP were incubated with anti-T7-tag antibody-conjugated agarose beads. Proteins bound to the beads (*IP*) and a 1% volume of total cell lysates (*input*) were analyzed by immunoblotting with the HRP-conjugated anti-FLAG and anti-T7 tag antibodies indicated on the *right* of each panel. The positions of the molecular mass markers (in kDa) are shown on the *left*. *D*, the number of nonciliated cells (%) in parental, Rab34-KO, and stable tagless Rab34(WT)-expressing or Rab34(S1A)-expressing Rab34-KO cells [*Rab34-KO* + *Rab34(WT)* or *Rab34(S1A)*] was counted after a 24-h serum starvation ($n > 50$ cells). *Error bars* indicate the S.E. of data from three independent experiments. ***, $p < 0.001$ (Tukey's test). *E*, the number of nonciliated cells (%) in parental, Rab34-KO, and stable FLAG-Rab34(WT), -Rab34(ΔN)-expressing Rab34-KO cells [*Rab34-KO* + *Rab34(WT)* or *Rab34(ΔN)*] was counted after a 24-h serum starvation ($n > 50$ cells). *Error bars* indicate the S.E. of data from three independent experiments. ***, $p < 0.001$; NS, not significant (Tukey's test). *F*, the protein expression level of FLAG-tagged Rab34(WT) and Rab34(ΔN) in *panel E* was analyzed by immunoblotting with the antibodies indicated on the *right* of each panel. The positions of the molecular mass markers (in kDa) are shown on the *left*. *G*, typical images of FLAG-Rab34 and GALNT2 or Arl13B in hTERT-RPE1 cells expressing FLAG-Rab34(S1A) or -Rab34(ΔN). *Top*, for GALNT2 staining, cells not subjected to serum starvation were fixed and stained with anti-GALNT2 antibody (*magenta*), anti-FLAG tag antibody (*green*), and DAPI (*blue*). *Bottom*, for Arl13B staining, cells were fixed after a 24-h serum starvation and then stained with antibodies against Arl13B (*magenta*) and FLAG (*green*). The arrows indicate FLAG-Rab34-positive primary cilia. *Scale bars*, 20 μm.

The known Rab34-interacting proteins are not required for ciliogenesis in hTERT-RPE1 cells

In the final set of experiments, we investigated the possible involvement of the known Rab34-interacting proteins, *i.e.* RILP, RILP-like 1 (RILP-L1), RILP-like 2 (RILP-L2) (30, 36, 37), Folliculin (FLCN) (38), and Munc13-2 (39), in ciliogenesis in hTERT-RPE1 cells. To narrow down the candidates, we first took advantage of the Rab34(S1A) mutant described above. Because Rab34(S1A) was able to support ciliogenesis (Fig. 6*D*), a Rab34 effector(s) that functions in ciliogenesis was expected to bind to Rab34(S1A). However, RILP and RILP-L1/L2 failed to interact with Rab34(S1A) (Fig. 6, *B* and *C*, and data not shown), indicating that the RILP-binding activity of Rab34 is not essential for ciliogenesis. Actually, knockdown of endogenous RILP in hTERT-RPE1 cells had no or little effect on ciliogenesis (Fig. 7*A*), and RILP-L1 and RILP-L2 have previously been shown to inhibit rather than promote ciliogenesis in hTERT-RPE1 cells (40). Therefore, we focused on FLCN, which had previously been shown to be associated with ciliopathy (41), and Munc13-2 in our subsequent analyses. An immunoblot analysis using specific antibodies showed that FLCN was endogenously expressed in hTERT-RPE1 cells (Fig. 7*B*), but no endogenous Munc13-2 expression was detected under our experimental conditions (Fig. S6*A*). Furthermore, transfection of a specific siRNA for Munc13-2 into hTERT-RPE1 cells had no effect on ciliogenesis (Fig. S6*B*), indicating that Munc13-2 is not a relevant effector in ciliogenesis. Finally, we knocked down endogenous FLCN in hTERT-RPE1 cells, and the results showed that FLCN-KD had no effect on ciliogenesis, even though the FLCN immunoreactive bands almost completely disappeared after treatment with two independent siRNAs (Fig. 7*B*). These findings taken together indicate that the known Rab34-interacting proteins, including RILP and FLCN, are not required for Rab34-regulated serum starvation-induced ciliogenesis in hTERT-RPE1 cells.

Discussion

In the present study, we performed a comprehensive knockdown screening for human Rabs that regulate ciliogenesis (Fig. 1), and, based on the results together with the results of KO analyses, we succeeded in identifying Rab34 as an essential Rab in serum starvation-induced ciliogenesis in hTERT-RPE1 cells (Fig. 1–3). Moreover, Rab34-KO had no effect on recruitment of IFT20, Rabin8, and Arl13B to centrioles or removal of CP110 from the mother centriole, but they inhibited axoneme elongation and extension of ciliary vesicles (Fig. 5*A*). These results suggest that Rab34 regulates the ciliary vesicle fusion step and/or the subsequent expansion step of serum starvation-induced ciliogenesis.

Although ~10 Rabs have been proposed to participate in ciliogenesis in previous studies (8, 13–18, 42–44), the results of knockdown or knockout of these Rabs in the present study demonstrated that none of the reported Rabs except Rab34 are essential for serum starvation-induced ciliogenesis, at least in hTERT-RPE1 cells under our experimental conditions (Fig. 1–3). Among the Rab-KO cells established in this study, only the Rab34-KO cells showed marked inhibition of ciliogenesis, and although Rab8/10-KO seemed to weakly inhibit ciliogenesis, the reduction was not statistically significant (Fig. 3). Nevertheless, we cannot rule out the possibility that Rabs other than Rab34 participate in ciliogenesis in other cell types or under different conditions (*e.g.* different upstream signals).

Intriguingly, when we checked the primary cilia in the cysts of recently established Rab-KO MDCK-II cells (27), we found that all of the Rab-KO cysts, including the Rab34-KO cysts, formed primary cilia in their luminal domain (Fig. 4, *C* and *D*, and Fig. S3). Thus, the mechanism of ciliogenesis in the two cell types is likely to be different. Actually, it has been proposed that ciliogenesis in polarized cells and in nonpolarized cells occurs in different pathways (45, 46). For example, the cilia in hTERT-RPE1 cells, NIH/3T3 cells, and MCF10A cells are induced by serum starvation, whereas the cilia in MDCK-II cells are induced during cyst growth in the absence of starvation. Thus, the upstream signals of ciliogenesis in hTERT-RPE1 and MDCK-II cells must be different, and Rab34 is specifically required for ciliogenesis in only certain cell types, such as hTERT-RPE1 cells, NIH/3T3 cells, and MCF10A cells. Consistent with this conclusion, Rab34-KO mice exhibited polydactyly, cleft lip, and cleft palate, but they did not have a polycystic kidney disease phenotype (23, 47), indicating that the primary cilia in their kidney cells are functionally normal.

Several questions regarding the function of Rab34 remain unanswered in this study. One of the important questions that must be answered in a future study concerns the function of the unique long N-terminal region of Rab34. Because no specific sequence in the switch II region of Rab34 is essential for serum starvation-induced ciliogenesis (Fig. 6 and Fig. S4), we hypothesized that the long N-terminal region contributes to recognition of an unidentified Rab34 effector that functions in ciliogenesis. Consistent with our hypothesis, N-terminal EGFP tagging of Rab34 significantly reduced its rescue efficiency (Fig. S2), presumably because fusion of a relatively large molecule, *e.g.* EGFP, to the N terminus of Rab34 partially impairs its interaction with an unidentified Rab34 effector. We used N-terminally GST (GSH *S*-transferase)-tagged or GBD (Gal4-binding domain)-tagged Rab34 as bait in our previous comprehensive screening for Rab effectors (34, 37, 48), but the screening methods we used are presumably inappropriate for identifying a Rab34 effector that functions in ciliogenesis. C-terminally tagged or untagged Rab34(S1A), which lacks binding activity toward RILP family members, would be useful in future screening for a novel Rab34 effector(s) in ciliogenesis. Another unanswered question concerns the cargo(s) Rab34 transports. One possible cargo is a component of SNARE complexes, because recruitment of an EHD1-binding protein, SNAP-29, to preciliary membranes is important for ciliogenesis, and a similar early-step ciliogenesis defect phenotype has been observed in EHD1-depleted cells (49). It is also unknown which membrane trafficking steps(s), *e.g.* budding, transport, docking, and fusion, Rab34 regulates. It had previously been shown that the main localization of Rab34 is the Golgi apparatus (30), and we confirmed its Golgi localization in the present study (Fig. 5*B*). The unique N-terminal region of Rab34 is not required for its Golgi localization, but no ciliary localization of Rab34(ΔN) was

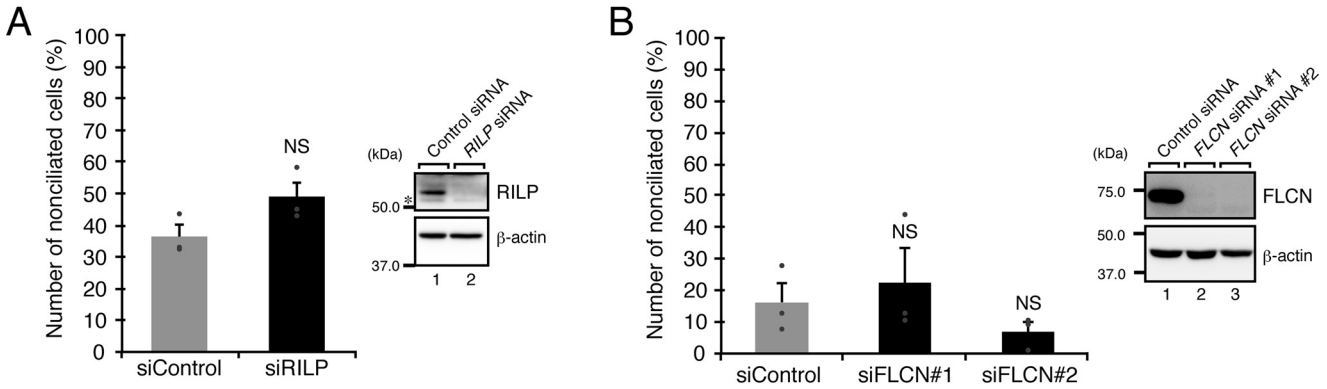

Figure 7. Two known Rab34-interacting proteins, RILP and FLCN, are not required for ciliogenesis in hTERT-RPE1 cells. *A*, the number of nonciliated control cells (*siControl*; 0.2 nM) and RILP-KD (*siRILP*; 0.2 nM) hTERT-RPE1 cells (%) was counted after a 24-h serum starvation ($n > 50$ cells). *Error bars* indicate the S.E. of data from three independent experiments. NS, not significant (Student's unpaired *t* test). The knockdown efficiency of RILP was evaluated by immunoblotting with the antibodies indicated on the *right* of each panel. Cells were harvested 48 h after transfection with control siRNA or *RILP* siRNA. The positions of the molecular mass markers (in kDa) are shown on the *left*. The *asterisk* indicates nonspecific bands of the anti-RILP antibody. *B*, the number of nonciliated control cells (*siControl*; 10 nM) and FLCN-KD (*siFLCN#1* and *#2*; 10 nM) hTERT-RPE1 cells (%) was counted after a 24-h serum starvation ($n > 50$ cells). *Error bars* indicate the S.E. of data from three independent experiments. NS, not significant (Tukey's test). The knockdown efficiency of FLCN was evaluated by immunoblotting with the antibodies indicated on the *right* of each panel. Cells were harvested 48 h after transfection with control siRNA or *FLCN* siRNA. *Lane 1* shows the results obtained with control cells, and *lanes 2* and *3* show the results obtained with the two FLCN-KD cells. The positions of the molecular mass markers (in kDa) are shown on the *left*.

observed, at least under our experimental conditions. Therefore, we assume that Rab34 regulates the budding/secretion step from the Golgi, the transport step of preciliary vesicles, and/or the fusion step of preciliary vesicles to form ciliary vesicles. Further extensive research will be necessary to answer all of the questions.

In summary, we found that Rab34 regulates early steps of serum starvation-induced ciliogenesis through its unique, previously uncharacterized N-terminal region and that its KO causes a loss of primary cilia even after serum starvation. In the future, it will be necessary to identify all of the membrane trafficking mechanisms responsible for Rab34-dependent ciliogenesis and determine the functional relationships between Rab34 and the previously reported Rabs, including Rab8 and Rab11, during ciliogenesis.

Experimental procedures

Antibodies

Anti-acetylated tubulin mouse mAb (no. T7451), anti-γ-tubulin mouse mAb (no. T5326), anti-FLAG tag (M2) mouse mAb (no. F1804), anti-GALNT2 rabbit polyclonal antibody (no. HPA011222), horseradish-peroxidase (HRP)-conjugated anti-T7 tag antibody (no. 69522), and HRP-conjugated anti-FLAG tag (M2) antibody (no. A8592) were obtained from Sigma-Aldrich. Anti-Arl13B rabbit polyclonal antibody (no. 17711-1-AP), anti-CP110 rabbit polyclonal antibody (no. 12780-1-AP), anti-IFT20 rabbit polyclonal antibody (no. 13615-1-AP), and anti-RILP rabbit polyclonal antibody (no. 13574-1-AP) were from Proteintech. Anti-Rab10 rabbit polyclonal antibody (no. 8127) and anti-FLCN (Folliculin) rabbit polyclonal antibody (no. 13697) were obtained from Cell Signaling Technology. Anti-Rab8 mouse mAb (no. 610845, BD Biosciences), anti-β-actin mouse mAb (no. G043, Applied Biological Materials), and anti-Munc13-2 (UNC13B) rabbit polyclonal antibody (no. ab97924, Abcam) were also obtained commercially. HRP-conjugated anti-mouse IgG goat polyclonal antibody (no. 1031-05) and anti-rabbit IgG goat polyclonal antibody (no. NA934) were from SouthernBiotech and GE Healthcare, respectively. Alexa Fluor 488/555/594/633-conjugated anti-mouse/rabbit IgG goat/donkey polyclonal antibodies were from Thermo Fisher Scientific. Anti-Rab11B, anti-Rab12, and anti-Rab34 rabbit polyclonal antibodies were prepared as described previously (27, 50).

siRNAs and plasmids

The sequences of the effective siRNAs against human Rabs are described in our previous study (20) (Table S1). The nomenclature of human Rabs is in accordance with the National Center for Biotechnology Information (NCBI) database rather than Itoh *et al.* (51); thus, four Rabs, *i.e.* Rab7B(42), Rab41(6D), Rab42(43), and Rab43(41), are named in this study as shown before parentheses and in our previous studies as shown in each set of parentheses. The siRNAs against human CEP164, RILP, FLCN (#1 and #2), and Munc13-2 were chemically synthesized by Nippon Gene (Toyama, Japan) (their target sequence is summarized in Table S1). The siRNA-resistant (SR) forms of human Rab34 (20), Rab34(S1A), Rab34^{SR}(KC/AA), and Rab34(ΔN) were prepared by conventional PCR techniques using the specific oligonucleotides shown in Table S1 as described previously (52) and subcloned into the pMRX-IRES-puro-EGFP, pMRX-IRES-bsr-EGFP-P2A, pEF-FLAG tag (53), and pGBD-C1 vectors (54). The cDNAs of mouse Rab34 (55), Rab34 (T66N), and Rab34(Q111L) (56) were subcloned into the pMRX-IRES-bsr-EGFP-P2A vector and pMRX-IRES-bsr vector, respectively. The P2A self-cleavage site (ATNFSLLKQAGDVEENPGP [25]) was inserted into the pMRX-IRES-bsr-EGFP vector by PCR using specific oligonucleotides (Table S1). The pMRX-IRES-puro/bsr-EGFP vectors are variants of the pMRX-IRES-puro/bsr vectors, which were donated by Dr. Shoji Yamaoka (Tokyo Medical and Dental University, Tokyo, Japan). pEF-FLAG-Rab34 and pEF-T7-RILP were prepared as described previously (34, 55). The cDNAs of mouse RILP-L1

and RILP-L2 (34) were subcloned into the pAct2 vector (Clontech/Takara Bio, Shiga, Japan).

The target sequences for human Rab8A/B-KO, Rab10-KO, Rab11B-KO, Rab12-KO, and Rab34-KO were designed by using CRISPR direct (https://crispr.dbcls.jp/) (summarized in Table S1). The annealed oligonucleotides of the Rab8A/B-KO and Rab11B-KO sense and antisense oligonucleotides were inserted into the pSpCas9(BB)-2A-bsr vector, a variant of pSpCas9(BB)-2A-puro (ID no. 48139) that was obtained by replacement of the puromycin-resistant gene (puro) by a blasticidin-resistant gene (bsr). The annealed oligonucleotides for Rab10-KO, Rab12-KO, and Rab34-KO were also inserted into the pSpCas9(BB)-2A-puro vector and pDonor-tBFP-NLS-Neo vector (Addgene ID no. 80766).

Cell culture and transfections

hTERT-RPE1 cells were cultured at 37 °C under 5% CO_2 in Dulbecco's modified Eagle medium–nutrient mixture F-12 (DMEM/F12) medium (Thermo Fisher Scientific) supplemented with 10% fetal bovine serum, 100 μg/ml streptomycin, and 100 unit/ml penicillin G. One day after plating, siRNAs and plasmids were transfected into hTERT-RPE1 cells by using Lipofectamine RNAi MAX for the siRNAs (concentrations are indicated in each figure legend) and Lipofectamine 2000 (Thermo Fisher Scientific) or Fugene6 (Promega) for the plasmids, each according to the manufacturer's instructions.

MCF10A cells were cultured at 37 °C under 5% CO_2 in DMEM/F12 medium supplemented with 5% horse serum, 50 ng/ml cholera toxin (Fujifilm Wako Pure Chemical, Osaka, Japan), 20 ng/ml epidermal growth factor (Fujifilm Wako Pure Chemical), 10 μg/ml insulin (Fujifilm Wako Pure Chemical), 500 ng/ml hydrocortisone (Fujifilm Wako Pure Chemical), 100 μg/ml streptomycin, and 100 unit/ml penicillin G. One day after plating, siRNAs (0.5 nM) were transfected into MCF10A cells by using Lipofectamine RNAiMAX according to the manufacturer's instructions. The same culture medium without the addition of horse serum and cholera toxin was used for serum starvation.

MDCK-II cells and NIH/3T3 cells were cultured at 37 °C under 5% CO_2 in DMEM supplemented with 10% fetal bovine serum, 100 μg/ml streptomycin, and 100 unit/ml penicillin G. Establishment of Rab-KO MDCK-II cells (listed in Fig. S3) and culture of three-dimensional cysts were performed as described previously (27). Rab34-KO NIH/3T3 cells were established in a similar manner (27). Plat-E cells were donated by Dr. Toshio Kitamura (The University of Tokyo, Tokyo, Japan). The plat-E cell culture and retrovirus infection were performed as described previously (57).

Establishment of CRISPR/Cas9 KO cell lines

hTERT-RPE1 cells that had been transfected with pSpCas9-bsr-Rab8A/B or -Rab11B were selected by exposure to 15 μg/ml blasticidin for ~48 h. hTERT-RPE1 cells that had been transfected with pSpCas9-puro-Rab10, -Rab12, or -Rab34 and pDonor-tBFP-NLS-Neo-Rab10, -Rab12, or -Rab34 were selected as described previously (58). Single clones were then selected by the limiting dilution method. KO cells were first checked for loss of target proteins by immunoblotting and then checked for genomic mutations by genomic PCR and sequencing of the PCR products as described previously (27).

Immunoblotting

hTERT-RPE1 cells were lysed in an SDS sample buffer (62.5 mM Tris-HCl, pH6.8, 2% 2-mercaptoethanol, 10% glycerol, and 0.02% bromphenol blue) in a lysis buffer (50 mM HEPES-KOH, pH7.2, 150 mM NaCl, 1 mM $MgCl_2$, and 1% Triton X-100). Cell lysates were subjected to SDS-PAGE, and proteins were transferred to PVDF membranes (Merck Millipore). The membranes were blocked with 1% or 5% skim milk and 0.1% Tween-20 in PBS and then reacted with specific primary antibodies. The reacted bands were visualized with appropriate HRP-conjugated secondary antibodies and detected by enhanced chemiluminescence.

Immunofluorescence analysis

hTERT-RPE1 cells, NIH/3T3 cells, and MCF10A cells that had been transfected with siRNAs or in which a *Rab* had been knocked out were fixed with 4% paraformaldehyde for 15 min at room temperature after a 24-h or 48-h serum starvation. After fixation, the cells were permeabilized with 0.3% Triton X-100 in PBS for 1 min and then stained with specific primary antibodies and appropriate Alexa Fluor 488/555/633-conjugated secondary antibodies. After a 7-day culture in collagen gel MDCK-II, cysts were fixed with 10% TCA for 15 min at room temperature and then stained with specific primary antibodies and appropriate Alexa Fluor 555/633-conjugated secondary antibodies. The immunostained cells were examined with a confocal fluorescence microscope (FV1000, FV1000-D; Olympus, Tokyo, Japan; and Dragonfly spinning disk scanning unit [Dragonfly200], Andor, Belfast, Northern Ireland).

Binding experiments

Coimmunoprecipitation assays of COS-7 cell lysates and yeast two-hybrid assays were performed as described previously (53, 59).

Statistical analysis

The data were statistically analyzed by performing Student's unpaired *t* test, Dunnett's test, or the Tukey-Kramer test. The single asterisk (*), double asterisks (**), and triple asterisks (***) in the graphs indicate p values of <0.05, <0.01, and <0.001, respectively. NS indicates not significant ($p > 0.05$).

Data availability

All presented data are contained within the article.

Acknowledgments—We thank Dr. Toshio Kitamura (The University of Tokyo) and Dr. Shoji Yamaoka (Tokyo Medical and Dental University) for kindly donating materials, Kan Etoh for preparing

plasmids, Takahide Matsui for valuable advice, Megumi Takada-Aizawa and Kazuyasu Shoji for technical assistance, and members of the Fukuda laboratory for valuable discussions.

Author contributions—M. E. O., K. O., Y. H., and M. F. conceptualization; M. E. O. and K. O. data curation; M. E. O. and K. O. formal analysis; M. E. O., Y. H., and M. F. funding acquisition; M. E. O. investigation; M. E. O., K. O., and M. F. writing-original draft; M. E. O., K. O., Y. H., and M. F. writing-review and editing; M. F. supervision.

Funding and additional information—This work was supported in part by Grant-in-Aid for Young Scientists from the Ministry of Education, Culture, Sports, Science and Technology (MEXT) of Japan Grant 20K15739 (to Y. H.), Grant-in-Aid for Scientific Research(B) from the MEXT Grant 19H03220 (to M. F.), Grant-in-Aid for Scientific Research on Innovative Areas Grant 15H01198 (to M. F.), by the Japan Science and Technology Agency (JST) CREST Grant JPMJCR17H4 (to M. F.), and by the Japan Society for the Promotion of Science (to M. E. O).

Conflict of interest—The authors declare that they have no conflicts of interest with the contents of this article.

Abbreviations—The abbreviations used are: bsr, blasticidin-resistant gene; EGFP, enhanced green fluorescent protein; FLCN, Folliculin; hTERT-RPE1, human telomerase reverse transcriptase retinal pigment epithelium 1; KC/AA, K115A/C116A; KD, knockdown; KO, knockout; puro, puromycin-resistant gene; MDCK, Madin-Darby canine kidney; NS, not significant; RILP, Rab interacting lysosomal protein; RILP-L1/L2, RILP-like 1/2; SR, siRNA resistant.

References

1. Satir, P., and Christensen, S. T. (2007) Overview of structure and function of mammalian cilia. *Annu. Rev. Physiol.* **69,** 377–400 CrossRef Medline
2. Reiter, J. F., and Leroux, M. R. (2017) Genes and molecular pathways underpinning ciliopathies. *Nat. Rev. Mol. Cell Biol.* **18,** 533–547 CrossRef Medline
3. Izawa, I., Goto, H., Kasahara, K., and Inagaki, M. (2015) Current topics of functional links between primary cilia and cell cycle. *Cilia* **4,** 12 CrossRef Medline
4. Sánchez, I., and Dynlacht, B. D. (2016) Cilium assembly and disassembly. *Nat. Cell Biol.* **18,** 711–717 CrossRef Medline
5. Sorokin, S. (1962) Centrioles rudimentary and smooth and the formation of cilia muscle by fibroblasts. *J. Cell Biol.* **15,** 363–377 CrossRef Medline
6. Sorokin, S. P. (1968) Reconstructions of centriole formation and ciliogenesis in mammalian lungs. *J. Cell Sci.* **3,** 207–230 Medline
7. Follit, J. A., Tuft, R. A., Fogarty, K. E., and Pazour, G. J. (2006) The intraflagellar transport protein IFT20 is associated with the Golgi complex and is required for cilia assembly. *Mol. Biol. Cell* **17,** 3781–3792 CrossRef Medline
8. Knödler, A., Feng, S., Zhang, J., Zhang, X., Das, A., Peränen, J., and Guo, W. (2010) Coordination of Rab8 and Rab11 in primary ciliogenesis. *Proc. Natl. Acad. Sci. U S A* **107,** 6346–6351 CrossRef Medline
9. Fukuda, M. (2008) Regulation of secretory vesicle traffic by Rab small GTPases. *Cell. Mol. Life Sci.* **65,** 2801–2813 CrossRef Medline
10. Stenmark, H. (2009) Rab GTPases as coordinators of vesicle traffic. *Nat. Rev. Mol. Cell Biol.* **10,** 513–525 CrossRef Medline
11. Hutagalung, A. H., and Novick, P. J. (2011) Role of Rab GTPases in membrane traffic and cell physiology. *Physiol. Rev.* **91,** 119–149 CrossRef Medline
12. Pfeffer, S. R. (2013) Rab GTPase regulation of membrane identity. *Curr. Opin. Cell Biol.* **25,** 414–419 CrossRef Medline
13. Yoshimura, S. I., Egerer, J., Fuchs, E., Haas, A. K., and Barr, F. A. (2007) Functional dissection of Rab GTPases involved in primary cilium formation. *J. Cell Biol.* **178,** 363–369 CrossRef Medline
14. Nachury, M. V., Loktev, A. V., Zhang, Q., Westlake, C. J., Peränen, J., Merdes, A., Slusarski, D. C., Scheller, R. H., Bazan, J. F., Sheffield, V. C., and Jackson, P. K. (2007) A core complex of BBS proteins cooperates with the GTPase Rab8 to promote ciliary membrane biogenesis. *Cell* **129,** 1201–1213 CrossRef Medline
15. Sato, T., Iwano, T., Kunii, M., Matsuda, S., Mizuguchi, R., Jung, Y., Hagiwara, H., Yoshihara, Y., Yuzaki, M., Harada, R., and Harada, A. (2014) Rab8a and Rab8b are essential for several apical transport pathways but insufficient for ciliogenesis. *J. Cell Sci.* **127,** 422–431 CrossRef Medline
16. Onnis, A., Finetti, F., Patrussi, L., Gottardo, M., Cassioli, C., Spanò, S., and Baldari, C. T. (2015) The small GTPase Rab29 is a common regulator of immune synapse assembly and ciliogenesis. *Cell Death Differ.* **22,** 1687–1699 CrossRef Medline
17. Pusapati, G. V., Kong, J. H., Patel, B. B., Krishnan, A., Sagner, A., Kinnebrew, M., Briscoe, J., Aravind, L., and Rohatgi, R. (2018) CRISPR screens uncover genes that regulate target cell sensitivity to the morphogen Sonic Hedgehog. *Dev. Cell* **44,** 113–129 CrossRef Medline
18. Gerondopoulos, A., Strutt, H., Stevenson, N. L., Sobajima, T., Levine, T. P., Stephens, D. J., Strutt, D., and Barr, F. A. (2019) Planar cell polarity effector proteins Inturned and Fuzzy form a Rab23 GEF complex. *Curr. Biol.* **29,** 3323–3330 CrossRef Medline
19. Sobajima, T., Yoshimura, S., Iwano, T., Kunii, M., Watanabe, M., Atik, N., Mushiake, S., Morii, E., Koyama, Y., Miyoshi, E., and Harada, A. (2014) Rab11a is required for apical protein localisation in the intestine. *Biol. Open* **4,** 86–94 CrossRef Medline
20. Aizawa, M., and Fukuda, M. (2015) Small GTPase Rab2B and its specific binding protein Golgi-associated Rab2B interactor-like 4 (GARI-L4) regulate Golgi morphology. *J. Biol. Chem.* **290,** 22250–22261 CrossRef Medline
21. Graser, S., Stierhof, Y. D., Lavoie, S. B., Gassner, O. S., Lamla, S., Le Clech, M., and Nigg, E. A. (2007) Cep164, a novel centriole appendage protein required for primary cilium formation. *J. Cell Biol.* **179,** 321–330 CrossRef Medline
22. Steger, M., Diez, F., Dhekne, H. S., Lis, P., Nirujogi, R. S., Karayel, O., Tonelli, F., Martinez, T. N., Lorentzen, E., Pfeffer, S. R., Alessi, D. R., and Mann, M. (2017) Systematic proteomic analysis of LRRK2-mediated Rab GTPase phosphorylation establishes a connection to ciliogenesis. *eLife* **6,** e31012 CrossRef
23. Xu, S., Liu, Y., Meng, Q., and Wang, B. (2018) Rab34 small GTPase is required for Hedgehog signaling and an early step of ciliary vesicle formation in mouse. *J. Cell Sci.* **131,** jcs213710 CrossRef
24. Breslow, D. K., Hoogendoorn, S., Kopp, A. R., Morgens, D. W., Vu, B. K., Kennedy, M. C., Han, K., Li, A., Hess, G. T., Bassik, M. C., Chen, J. K., and Nachury, M. V. (2018) A CRISPR-based screen for Headgehog signaling provides insights into ciliary function and ciliopathies. *Nat. Genet.* **50,** 460–471 CrossRef Medline
25. Kim, J. H., Lee, S. R., Li, L. H., Park, H. J., Park, J. H., Lee, K. Y., Kim, M. K., Shin, B. A., and Choi, S. Y. (2011) High cleavage efficiency of a 2A peptide derived from porcine teschovirus-1 in human cell lines, zebrafish and mice. *PLoS ONE* **6,** e18556 CrossRef Medline
26. Homma, Y., and Fukuda, M. (2016) Rabin8 regulates neurite outgrowth in both GEF-activity-dependent and -independent manners. *Mol. Biol. Cell* **27,** 2107–2118 CrossRef Medline
27. Homma, Y., Kinoshita, R., Kuchitsu, Y., Wawro, P. S., Marubashi, S., Oguchi, M. E., Ishida, M., Fujita, N., and Fukuda, M. (2019) Comprehensive knockout analysis of the Rab family GTPases in epithelial cells. *J. Cell Biol.* **218,** 2035–2050 CrossRef Medline
28. Spektor, A., Tsang, W. Y., Khoo, D., and Dynlacht, B. D. (2007) Cep97 and CP110 suppress a cilia assembly program. *Cell* **130,** 678–690 CrossRef Medline

29. Larkins, C. E., Aviles, G. D. G., East, M. P., Kahn, R. A., and Caspary, T. (2011) Arl13b regulates ciliogenesis and the dynamic localization of Shh signaling proteins. *Mol. Biol. Cell* **22,** 4694–4703 CrossRef Medline
30. Wang, T., and Hong, W. (2002) Interorganellar regulation of lysosome positioning by the Golgi apparatus through Rab34 interaction with Rab-interacting lysosomal protein. *Mol. Biol. Cell* **13,** 4317–4332 CrossRef Medline
31. Kloer, D. P., Rojas, R., Ivan, V., Moriyama, K., van Vlijmen, T., Murthy, N., Ghirlando, R., van der Sluijs, P., Hurley, J. H., and Bonifacino, J. S. (2010) Assembly of the biogenesis of lysosome-related organelles complex-3 (BLOC-3) and its interaction with Rab9. *J. Biol. Chem.* **285,** 7794–7804 CrossRef Medline
32. Tamura, K., Ohbayashi, N., Ishibashi, K., and Fukuda, M. (2011) Structure-function analysis of VPS9-ankyrin-repeat protein (Varp) in the trafficking of tyrosinase-related protein 1 in melanocytes. *J. Biol. Chem.* **286,** 7507–7521 CrossRef Medline
33. Etoh, K., and Fukuda, M. (2015) Structure-function analyses of the small GTPase Rab35 and its efffector protein centaurin-β2/ACAP2 during neurite outgrowth of PC12 cells. *J. Biol. Chem.* **290,** 9064–9074 CrossRef Medline
34. Matsui, T., Ohbayashi, N., and Fukuda, M. (2012) The Rab interacting lysosomal protein (RILP) homology domain functions as a novel effector domain for small GTPase Rab36: Rab36 regulates retrograde melanosome transport in melanocytes. *J. Biol. Chem.* **287,** 28619–28631 CrossRef Medline
35. Homma, Y., Hiragi, S., and Fukuda, M. (2020) Rab family of small GTPases: an updated view on their regulation and functions. *FEBS J.* CrossRef
36. Wang, T., Wong, K. K., and Hong, W. (2004) A unique region of RILP distinguishes it from its related proteins in its regulation of lysosomal morphology and interaction with Rab7 and Rab34. *Mol. Biol. Cell* **15,** 815–826 CrossRef Medline
37. Fukuda, M., Kanno, E., Ishibashi, K., and Itoh, T. (2008) Large scale screening for novel Rab effectors reveals unexpected broad Rab binding specificity. *Mol. Cell. Proteomics* **7,** 1031–1042 CrossRef Medline
38. Starling, G. P., Yip, Y. Y., Sanger, A., Morton, P. E., Eden, E. R., and Dodding, M. P. (2016) Folliculin directs the formation of a Rab34-RILP complex to control the nutrient-dependent dynamic distribution of lysosomes. *EMBO Rep.* **17,** 823–841 CrossRef Medline
39. Goldenberg, N. M., and Silverman, M. (2009) Rab34 and its effector munc13-2 constitute a new pathway modulating protein secretion in the cellular response to hyperglycemia. *Am. J. Physiol. Cell Physiol.* **297,** C1053–C1058 CrossRef Medline
40. Schaub, J. R., and Stearns, T. (2013) The Rilp-like proteins Rilpl1 and Rilpl2 regulate ciliary membrane content. *Mol. Biol. Cell* **24,** 453–464 CrossRef Medline
41. Luijten, M. N. H., Basten, S. G., Claessens, T., Vernooij, M., Scott, C. L., Janssen, R., Easton, J. A., Kamps, M. A. F., Vreeburg, M., Broers, J. L. V., van Geel, M., Menko, F. H., Harbottle, R. P., Nookala, R. K., Tee, A. R., *et al.* (2013) Birt-Hogg-Dube syndrome is a novel ciliopathy. *Hum. Mol. Genet.* **22,** 4383–4397 CrossRef Medline
42. Dhekne, H. S., Yanatori, I., Gomez, R. C., Tonelli, F., Diez, F., Schüle, B., Steger, M., Alessi, D. R., and Pfeffer, S. R. (2018) A pathway for Parkinson's disease LRRK2 kinase to block primary cilia and sonic hedgehog signaling in the brain. *eLife* **7,** e40202 CrossRef
43. Wang, G., Hu, H. B., Chang, Y., Huang, Y., Song, Z. Q., Zhou, S. B., Chen, L., Zhang, Y. C., Wu, M., Tu, H. Q., Yuan, J. F., Wang, N., Pan, X., Li, A. L., Zhou, T., *et al.* (2019) Rab7 regulates primary cilia disassembly through cilia excision. *J. Cell Biol.* **218,** 4030–4041 CrossRef Medline
44. Kuhns, S., Seixas, C., Pestana, S., Tavares, B., Nogueira, R., Jacinto, R., Ramalho, J. S., Simpson, J. C., Andersen, J. S., Echard, A., Lopes, S. S., Barral, D. C., and Blacque, O. E. (2019) Rab35 controls cilium length, function and membrane composition. *EMBO Rep.* **20,** e47625 CrossRef Medline
45. Rohatgi, R., and Snell, W. J. (2010) The ciliary membrane. *Curr. Opin. Cell Biol.* **22,** 541–546 CrossRef Medline
46. Benmerah, A. (2013) The ciliary pocket. *Curr. Opin. Cell Biol.* **25,** 78–84 CrossRef Medline
47. Dickinson, M. E., Flenniken, A. M., Ji, X., Teboul, L., Wong, M. D., White, J. K., Meehan, T. F., Weninger, W. J., Westerberg, H., Adissu, H., Baker, C. N., Bower, L., Brown, J. M., Caddle, L. B., Chiani, F., *et al.*, (2016) High-throughput discovery of novel developmental phenotypes. *Nature* **537,** 508–514 CrossRef Medline
48. Kanno, E., Ishibashi, K., Kobayashi, H., Matsui, T., Ohbayashi, N., and Fukuda, M. (2010) Comprehensive screening for novel Rab-binding proteins by GST pull-down assay using 60 different mammalian Rabs. *Traffic* **11,** 491–507 CrossRef Medline
49. Lu, Q., Insinna, C., Ott, C., Stauffer, J., Pintado, P. A., Rahajeng, J., Baxa, U., Walia, V., Cuenca, A., Hwang, Y.-S., Daar, I. O., Lopes, S., Lippincott-Schwartz, J., Jackson, P. K., Caplan, S., *et al.* (2015) Early steps in primary cilium assembly require EHD1/EHD3-dependent ciliary vesicle formation. *Nat. Cell Biol.* **17,** 228–240 CrossRef Medline
50. Matsui, T., Itoh, T., and Fukuda, M. (2011) Small GTPase Rab12 regulates constitutive degradation of transferrin receptor. *Traffic* **12,** 1432–1443 CrossRef Medline
51. Itoh, T., Satoh, M., Kanno, E., and Fukuda, M. (2006) Screening for target Rabs of TBC (Tre-2/Bub2/Cdc16) domain-containing proteins based on their Rab-binding activity. *Genes Cells* **11,** 1023–1037 CrossRef Medline
52. Fukuda, M., Kojima, T., Aruga, J., Niinobe, M., and Mikoshiba, K. (1995) Functional diversity of C2 domains of synaptotagmin family: mutational analysis of inositol high polyphosphate binding domain. *J. Biol. Chem.* **270,** 26523–26527 CrossRef Medline
53. Fukuda, M., Kanno, E., and Mikoshiba, K. (1999) Conserved N-terminal cysteine motif is essential for homo- and heterodimer formation of synaptotagmins III, V, VI, and X. *J. Biol. Chem.* **274,** 31421–31427 CrossRef Medline
54. James, P., Halladay, J., and Craig, E. A. (1996) Genomic libraries and a host strain designed for highly efficient two-hybrid selection in yeast. *Genetics* **144,** 1425–1436 Medline
55. Fukuda, M., Kuroda, T. S., and Mikoshiba, K. (2002) Slac2-a/melanophilin, the missing link between Rab27 and myosin Va: implications of a tripartite protein complex for melanosome transport. *J. Biol. Chem.* **277,** 12432–12436 CrossRef Medline
56. Ishida, M., Ohbayashi, N., Maruta, Y., Ebata, Y., and Fukuda, M. (2012) Functional involvement of Rab1A in microtubule-dependent anterograde melanosome transport in melanocytes. *J. Cell Sci.* **125,** 5177–5187 CrossRef Medline
57. Morita, S., Kojima, T., and Kitamura, T. (2000) Plat-E: an efficient and stable system for transient packaging of retroviruses. *Gene Ther.* **7,** 1063–1066 CrossRef Medline
58. Katoh, Y., Michisaka, S., Nozaki, S., Funabashi, T., Hirano, T., Takei, R., and Nakayama, K. (2017) Practical method for targeted disruption of cilia-related genes by using CRISPR/Cas9-mediated, homology-independent knock-in system. *Mol. Biol. Cell* **28,** 898–906 CrossRef Medline
59. Kobayashi, H., Etoh, K., Marubashi, S., Ohbayashi, N., and Fukuda, M. (2015) Measurement of Rab35 activity with the GTP-Rab35 trapper RBD35. *Methods Mol. Biol.* **1298,** 207–216 CrossRef Medline